Upcycling Byproducts from Insect (Fly Larvae and Mealworm) Farming into Chitin Nanofibers and Films

Eva Pasquier, Marco Beaumont, Bruno Mattos, Caio Otoni, Armin Winter, Thomas Rosenau, Mohamed Naceur Belgacem, Orlando Rojas, Julien Bras

Pasquier, Eva; Beaumont, Marco; Mattos, Bruno D.; Otoni, Caio G.; Winter, Armin; Rosenau, Thomas; Belgacem, Mohamed Naceur; Rojas, Orlando J.; Bras, Julien

Upcycling Byproducts from Insect (Fly Larvae and Mealworm) Farming into Chitin Nanofibers and Films

Published in:
ACS Sustainable Chemistry and Engineering

DOI:
10.1021/acssuschemeng.1c05035

Published: 11/10/2021

Document Version
Peer-reviewed accepted author manuscript, also known as Final accepted manuscript or Post-print

Upcycling Byproducts from Insect (Fly Larvae and Mealworm) Farming into Chitin Nanofibers and Films

Eva Pasquier[a,b], Marco Beaumont[c], Bruno D. Mattos[b], Caio G. Otoni[d], Armin Winter[e], Thomas Rosenau[c,f], Mohamed Naceur Belgacem[a,g], Orlando J. Rojas[b,h,], Julien Bras[a]*

[a] *Université Grenoble Alpes, CNRS, Grenoble INP (*Institute of Engineering*), LGP2, F-38000 Grenoble, France*

[b] *Department of Bioproducts and Biosystems, School of Chemical Engineering, Aalto University, P.O. Box 16300, Aalto, Espoo FIN-00076, Finland*

[c] *University of Natural Resources and Life Sciences, Vienna (BOKU), Institute of Chemistry of Renewable Resources, Konrad-Lorenz-Str. 24, A-3430 Tulln, Austria*

[d] *Department of Materials Engineering, Federal University of São Carlos (UFSCar), Rod. Washington Luís km 235, São Carlos, SP 13565-905, Brazil*

[e] *University of Natural Resources and Life Sciences, Vienna, Institute of Wood Technology and Renewable Materials, Konrad Lorenz Straße 24, A-3430 Tulln an der Donau*

[f] *Johan Gadolin Process Chemistry Centre, Åbo Akademi University, Porthansgatan 3, Åbo/Turku FI-20500, Finland.*

[g] *Institut Universitaire de France (IUF), 75000 Paris, France*

[h] *Bioproducts Institute, Departments of Chemical and Biological Engineering, Chemistry and Wood Science, University of British Columbia, 2360 East Mall, Vancouver, BC V6T 1Z3, Canada*

*Corresponding author: Julien.bras@grenoble-inp.fr

KEYWORDS: Nanochitin, insect farming, environmental footprint, *Hermetia illucens*, *Tenebrio molitor*, future foods

ABSTRACT

Nowadays environmental concerns make us rethink the way we live and eat. In this regard, alternative protein sources are emerging; among them, insects are some of the most promising alternatives. Insect farming is still an infant industry, and to improve its profitability and environmental footprint, valorization of the by-products will be a key step. Chitin as main polysaccharide in the exoskeleton of insects has a great potential in this regard and can be processed into high value-added materials. In this study, we extracted and fibrillated chitin fibers from fly larvae (*Hermetia illucens*) and compared it with commercial chitin from shrimp shells. A mix of chitin and cellulose fibers was also extracted from mealworm farming waste. The purified chitinous fibers from different sources had similar chemical structures as shown by FTIR and NMR spectroscopies. After mechanical fibrillation, the nanostructures of the different nanofibers were similar with heights between 9 and 11 nm. Chitin nanofibers (ChNF) from fly larvae presented less non-fibrillated fiber bundles than the shrimp-derived analogue, pointing towards a lower recalcitrance of the fly larvae. ChNF suspensions underwent different film-forming protocols leading to films with tensile strengths of 83 ± 7 and 71 ± 4 MPa for ChNF from shrimp and fly, respectively. While the effect of chitin source on the mechanical properties of the films was demonstrated to be negligible, the presence of cellulose nanofibers closely mixed with ChNF in the case of mealworm led to films twice as tough. Our results show for the first time the feasibility of producing ChNF from insect industry byproducts with high potential for valorization and integral use of biomass.

INTRODUCTION

Today's environmental crisis has urged scientist to find alternatives to conventional sources of proteins. With their high protein content, insects are promising food[1–3] and feed[4] alternatives, and their composition also includes high amounts of lipids and structural polysaccharides, notably chitin. Insects are considered as future foods to potentially replace conventional animal sources of protein,[2] also having great advantages regarding current environmental issues. One reason is the incredibly high protein yield per production space in comparison to other protein sources, mainly due to the possibility of vertical farming: One kilogram of edible protein from mealworm requires 18 m^2, differing in one order of magnitude from beef cattle (200 m^2/kg).[5] In addition, the amount of water needed for insect farming is low as some insects can grow without water and can be fed in a very sustainable manner, *e.g.* with crop waste.[6] Moreover, it was shown that frass from mealworm larvae farming has similar fertilizing potential as conventional mineral fertilizers.[7] All these arguments explain the advancement of insect farming. Although the pertinent business models are still under development, it is obvious that valorization of all components is needed to meet the demands of sustainable biorefinery approaches.[8] Chitin is one of the insects´ main components, representing 5 to 10% of their dry matter.[9,10] Chitin possesses a high potential in agriculture, waste treatment, cosmetic, healthcare, food, or materials application and its utilization could further enhance the sustainability of insect farming. The chitin present in the insects´ body, larvae, or shells can be readily separated from the protein-rich fractions. Caligiani et al. showed that black soldier fly prepupae can be integrated in a biorefinery approach as source of proteins, lipids, and chitin.[11] In addition, during the different life stages (larvae, pupae, prepupae, adult), insects molt, leaving behind shells (exoskeletons) as a chitin-rich side stream[12,13] that could be directly used for chitin extraction.

Colloidal nanofibers can be obtained from chitinous biomass by mechanical treatment at high pressure or sonication of purified chitin suspensions.[14] Chitin nanofibers (ChNFs) have a tremendous potential in the fabrication of materials given their unique properties. Compared to nanocellulose, nanochitin is less hydrophilic and can bear cationic surface groups due to deacetylation of the *N*-acetyl moieties, which support, *via* electrostatic repulsion, the individualization into nanofibers. Moreover, the presence of primary amino groups on the fibril surface after partial deacetylation opens many doors for chemical functionalization absent in nanocelluloses. When protonated, these groups also offer the opportunity of physical functionalization through the electrostatic toolbox and render ChNF suspensions colloidally stable. Its fibrillar nature, biodegradability as well as natural cationic surface make deacetylated chitin/chitosan a promising, versatile building block for material development, as demonstrated in composites,[15] membranes,[16] platforms for waste water treatment, and emulsion stabilization.[17]

Many studies have shown the extraction of nanochitin from shrimps, crabs,[18] squid pen,[19] mushrooms,[20] and *Riftia tube*,[21] but the production and comparison of ChNFs from different insect sources has been overlooked so far. In fact, chitin has been extracted from insects, but only few comparisons between crustacean and insect chitin have been reported and no nanofibers have been obtained from insect chitin.[12,22–24] The chitins possess similar chemical structures, crystalline arrays, and thermal properties,[23] but differences in morphology, in particular the accessibility of the fibers, were noted.[12,22] Also, given the unique chemical composition and therefore recalcitrance of each chitin source (either from crustaceans or insects), the extraction and purification processes should be tuned accordingly. Whereas crustacean shells are mainly composed of calcium carbonate, exoskeletons of insects contain relatively more proteins and lipids. The conventional demineralization/deproteinization steps

should therefore be adapted.[25] Fungi are another source of chitin, from which ChNFs have been extracted, though with low purity due to glucans present on the fibers´ surface.[26]

In this work, we have studied the effects of the chitinous raw material on the purification of chitin and the subsequent isolation of nanofibers and their properties. ChNFs were produced from chitin of black soldier fly (*Hermetia illucens*) larvae and chitinous waste from mealworm (*Tenebrio molitor*) farming. These two species are among the most promising insects for industrial farming,[9] being both considered as future foods,[2] which has triggered several companies (*e.g.,* Ynsect, Alpha Chitin, InnovaFeed, Enterra, Die Wurm Farm, and Protix) to start efforts at pilot and industrial scales. In addition, mealworm has recently been considered safe for human consumption as food by the European Food Safety Authority (EFSA).[27] In our work, purification of the chitins from different sources was followed by mechanical disintegration to form nanofibers (see **Figure 1**). Comparisons of the structural properties of the extracted nanofibers and their ability to form self-standing films are presented. The influence of impurities was also considered and discussed. With this work we hope to encourage efforts to upcycle insect farming waste into high-performance building blocks for colloidal and solid-state materials.

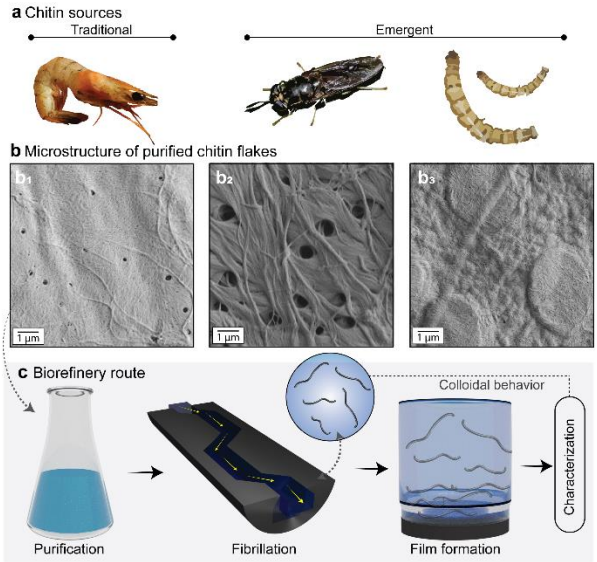

Figure 1: Different chitin sources used in this study (**a**). Microstructure of the purified chitin fibers from shrimp (**b1**), fly larvae (**b2**) and mealworm (**b3**) shown by SEM images (**b**). Different process steps conducted before characterization of the materials (**c**).

RESULTS AND DISCUSSION

Analysis of the purified materials

We first compared the properties of chitin fibers obtained from the larvae and residual biomass of emerging farming of fly (*Hermetia illucens*) larvae and mealworm (*Tenebrio molitor*) with those of chitin purified from shrimp shell, a conventional commercial source of this polysaccharide. We analyzed the chemical composition and purity of the raw materials using Fourier-Transform Infrared (FTIR) and solid-state ^{13}C Nuclear Magnetic Resonance (NMR) spectroscopies **(Figure S1** and **S2**). The results were also used to adapt the conditions of purification applied to each chitinous biomass (fly, mealworm, and shrimp). According to the NMR spectra both fly and shrimp raw chitin samples did not contain significant amount of proteins or lipids while that from the mealworm production contained considerable amounts of lipids and proteins (**Figure S2**). This is also visible in the IR spectrum of the mealworm chitin which displayed a significantly lower intensity of the C–O IR band at ca. 1000 cm^{-1} (corresponding mostly to polysaccharide moieties, see Table S1 for further details) than the other raw materials, whereas the intensity of C=O band at 1450-1700 cm^{-1} was similar (**Figure S1**). Moreover, NMR indicated that the mealworm waste sample was a mixture of chitin and cellulose. The cellulose fraction originated from the cereal-based feed of the mealworm (residual husk as feed leftover) which was mixed with the mealworm exuviae. The inorganic residues in the samples were analyzed thermogravimetrically: the ash contents of the as-received materials were 0.3, 4.0, and 4.8 wt%, for S-Ch, F-Ch, and W-Fiber, respectively.

The conventional demineralization, deproteinization, and bleaching steps that are usually applied for crustacean shells were carried out using similar concentrations and temperatures, but the time was adapted to each source following the optimization method of Percot et al.[28] A mild demineralization step with 0.25 M HCl at room temperature was followed by a treatment with 1M NaOH at 50 °C between 4 and 24 h, depending on the source, and sodium chlorite bleaching cycles (2 h at 80 °C). Although the fly and shrimp raw chitins were of considerable purity, these steps were required to remove remaining inorganic and protein contaminants. The purification yields were 90% for the shrimp and 68% for the fly. For the mealworm sample, we used a different protocol and first extracted the lipid fraction with *n*-hexane. After extraction, we applied the same protocol as for the other chitin samples but added an alkaline purification step due to the high protein content of the material, applying 1 M NaOH for 1 h at 70 °C between two bleaching cycles. The yield after extraction was 11%.

The solid-state ^{13}C NMR spectra of all chitin samples after purification are shown in **Figure 2a**. The chitins extracted from shrimp (S-Chitin) and fly (F-Chitin) were almost identical, apart from protein traces in the fly sample (in the range of 30 ppm).[29] Comparable resonances assigned to proteins were also present in the NMR spectra of the mealworm sample (W-Fiber) in which the cellulose fraction was clearly identified (**Figure S3**). The amount of cellulose in the sample was estimated to approx. 44 wt% (50 mol%) by comparing the peak intensity of the C2 of the chitin fraction at around 55 ppm to the combined C1 peak intensity of chitin and cellulose at about 102 ppm.

The ash contents after purification of the three materials were 0.1%, 1.4%, and 1.2% for S-Ch, F-Ch, and W-Fiber, respectively. Although the initial ash content in every sample was already low (0.3, 4.0, and 4.8 wt%, respectively), it further decreased through removal of inorganic residues.

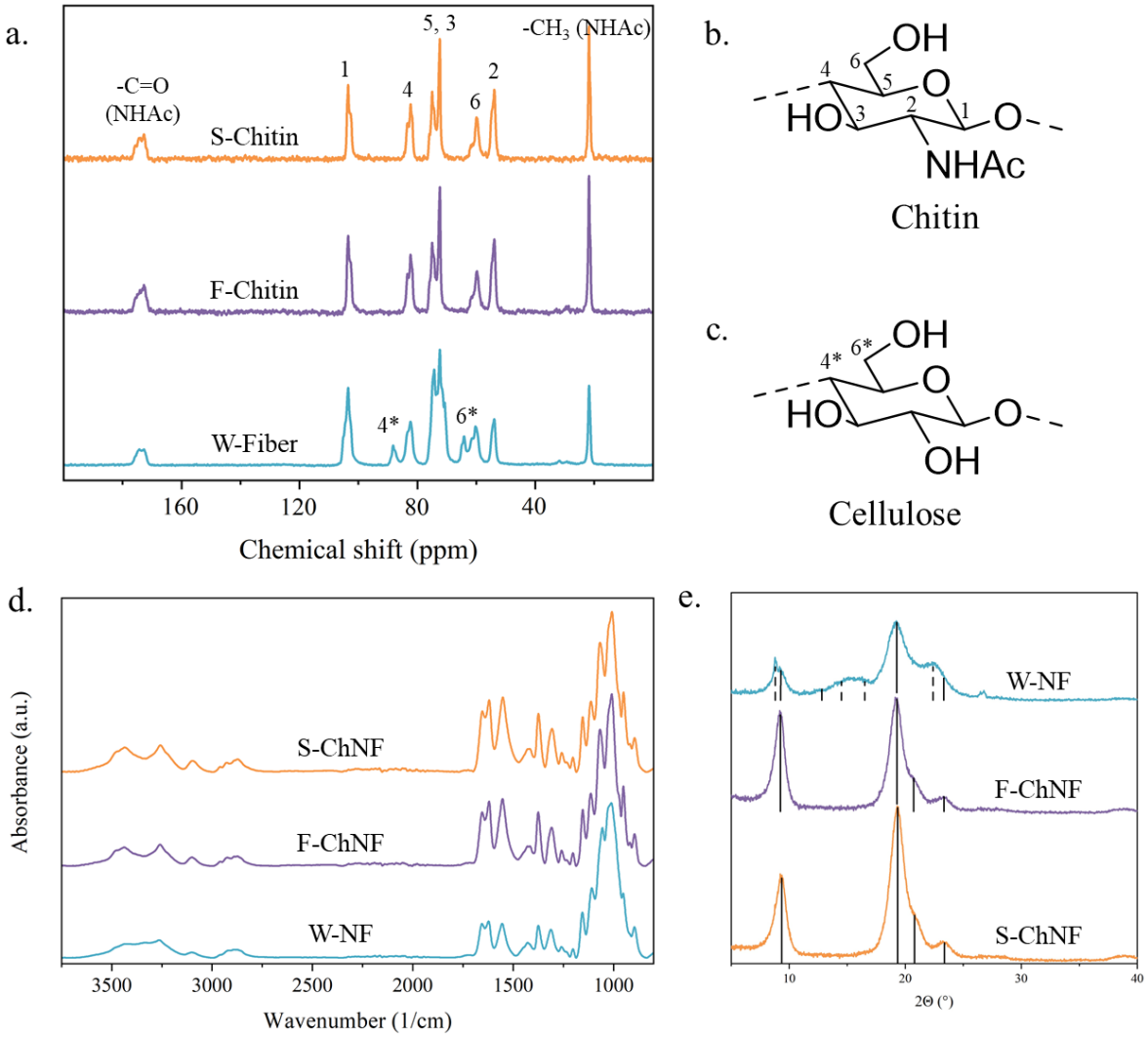

Figure 2. ^{13}C NMR spectra of the purified fibers from shrimp (S-Chitin), fly (F-Chitin), and mealworm (W-Fiber) (**a**), the latter encompassing cellulose (**c**) in addition to chitin (**b**, respective carbons are numbered and assigned to the NMR spectra). FTIR (**d**) and XRD (**e**) spectra of the dried nanofibers (S-ChNF, F-ChNF, and W-NF). Solid lines in the diffractograms indicate chitin and dashed lines cellulose peaks.

Structural analysis of the chitin nanofibers

After purification, the chitins were processed into nanofibers by fibrillation under mild acidic conditions. The suspensions were passed six times through a microfluidizer at 1500 bar without

any chemical pretreatment. After defibrillation, white gel-like nanofiber suspensions were obtained from S-chitin (S-ChNF), fly larvae (F-ChNF), and mealworm exuviae (W-NF).

FTIR of the fibrillated nanofibers allowed tracking possible chemical changes arising from the purification and processing steps (see **Table S1** for peak assignment). **Figure 2d** shows that the three materials have the fingerprint regions of glucopyranoxylamine (and glucopyranose in case of W-NF) rings in the 1000-1155 cm^{-1} region related to C–O and C–O–C bonds.[30] The amide I and II bands of chitin (1555, 1620, and 1660 cm^{-1}) were also present in all of the three different materials, although having lower intensity in W-NF due to the presence of cellulose. The peaks at 1630 and 1530 cm^{-1}, related to amide bonds in proteins,[23] were predominant in the raw mealworm samples, but were remarkably less intense in W-NF, indicating efficient deproteinization (see **Figure S1**).

Figure 2e displays the XRD spectra of the three different nanofibers. The typical pattern of α-chitin was present in all samples, with a peak of maximum intensity at 19.2° and a second peak at 9.2°, which is in accordance with results reported for insect chitin.[31] The crystallinity was found to be 94% and 93% for S-ChNF and F-ChNF, respectively. Peaks from both cellulose and chitin were visible in the XRD profile of W-NF. The peaks at 14.5°, 16.5°, and 22.5° corresponded to the cellulose Iα planes (100), (010), and (110), respectively,[32] and those at 9.3°, 12.8°, 19.3°, 20.9°, and 23.4° to the α-chitin planes (020), (101), (110), (120), and (130), respectively.[33] Due to the mix of cellulose and chitin and the fact that peaks were overlapping, it was not possible to calculate the crystallinity index of W-NF.

The surface chemistry of the nanofibers with regard to charged groups was assessed by zeta potential measurements at different pH. S-ChNF and F-ChNF are negatively charged at basic pH and positively charged at acidic pH, with an isoelectric point of approx. 6 (see **Table 1** and **Figure S4**). The negative zeta-potential of F-ChNF at pH 7 could be explained by the higher

fibrillation degree of the F-ChNF and the high variation of zeta-potential around the iso-electric points. The presence of acetamide groups on the surface of the nanofibers, and in particular amino groups by deacetylation, leads to positively charged nanofibers in acidic media. The positive charge and the presence of amine are advantages of ChNF over their cellulosic counterparts, as this opens many opportunities regarding functionalization or interaction with molecules containing carboxylic acids or other anionic moieties.[34] Further deacetylation, which is usually done prior to defibrillation, allows tuning the amine content on the surface of ChNFs.[35] Although W-NF was a mix of chitin and cellulose, it displayed a negatively charged surface. The cellulosic contribution was predominant in the blend, leading to a net negative zeta potential throughout the studied pH range. Cellulose fibers are naturally negatively charged at a wide pH range because of the presence of residual hemicelluloses.[36] Classically, the zeta potential of cellulose fibers ranges from -20 to -50 mV depending on the source; hence the value of -7.2 mV confirms a mix of positive and negative charges from chitin and cellulose, respectively.

To further study the surface charge of the nanofibers, conductometric titration was performed and the degree of acetylation was determined. The surface charge densities of S-ChNF, F-ChNF, and W-NF were 215 ± 13, 209 ± 5 and 293 ± 18 μmol/g, respectively. Associated degrees of *N*-acetylation (DA) were 96%, 95%, and ca. 90% for S-ChNF, F-ChNF, and W-NF, respectively. The DA of W-NF was estimated for its chitin fraction. From the calculated DA (conductometric titration), displayed in **Table 1**, we conclude a relatively low content of primary amine groups in the nanofibers, probably due to the mild purification steps. This is in accordance with Ifuku et al., who measured a DA of 95% for non-deacetylated ChNFs from crab[37] and Huet et al., who calculated a DA of 93% for chitin from insects.[23] The approximated DA of W-NF was slightly lower, which might be reasoned by the additional and more severe caustic treatment.

Table 1. Zeta potential at different pH and charge content measured by conductometric titration and associated degree of *N*-acetylation. *Degree of *N*-acetylation of W-NF was estimated for its chitin fraction.

	Zeta potential pH 3	Zeta potential pH 7	Charge density	Degree of *N*-acetylation
	mV	mV	μmol/g	-
S-ChNF	27 ± 3	2 ± 2	215 ± 13	95.7 ± 0.3%
F-ChNF	23 ± 3	-10.6 ± 0.5	209 ± 5	95.1 ± 0.1%
W-NF	-7.2 ± 0.7	-18 ± 1	293 ± 18	≈ 90%*

The morphology of the chitinous nanofibers was investigated by AFM **(Figure 3a-c)**, from which the height distribution (**Figure 3d-f**) was obtained. Overall, well separated nanofibers, with average height between 4 and 35 nm were obtained, regardless of the chitin source. Additionally, the transmittance of the aqueous suspensions of nanofibers was measured at pH 3 and 0.1 wt% concentration to gain further insights into their colloidal behavior, in terms of aggregation and stability (**Table 2**). A remarkable difference in transmittance was observed between S-ChNF (15.2 ± 0.6%) and F-ChNF (28.7 ± 0.8%), indicating that the nanofibers from fly larvae were fibrillated to a greater extent, even though they showed seemingly similar morphologies in the AFM images (**Figure 3)**. To confirm such difference, the ratio between fine and coarse fractions in the suspensions was measured gravimetrically (**Table 2**). A higher amount of fine fraction, meaning smaller nanofibers that remain in suspension under centrifugal forces, was measured for F-ChNF (35 ± 2%) compared to S-ChNF (24 ± 10%). Chitins from insects have been reported to be more accessible than those from crustacean,[22,38] which could have facilitated the fibrillation, explaining the difference.

To increase the density of repulsive charges, ChNF suspensions are usually processed at pH 3 to protonate the primary amino groups and kinetically stabilize the suspensions. Due to the mix of cellulose and chitin nanofibers in W-NF, the stability of this suspension might differ with pH, as shown by the zeta potential. To investigate the pH-dependency in the aggregation phenomena of the W-NF suspension, we measured the transmittance at pH 3 and 7. The transmittance at pH 3 (18.2 ± 0.5%) was slightly lower than at pH 7 (20.9 ± 0.5%), which indicates no remarkable aggregation of the nanofibers at pH 3.

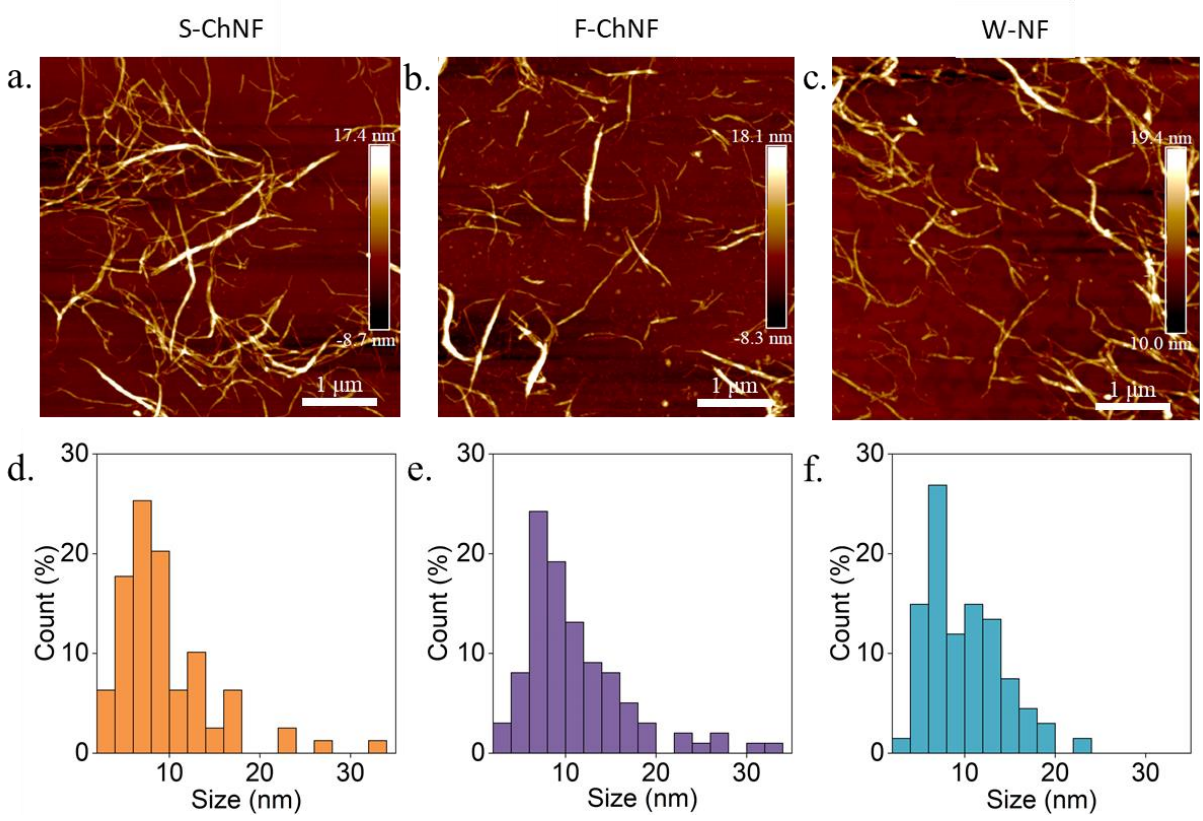

Figure 3. AFM images of S-ChNF (**a**), F-ChNF (**b**), and W-NF (**c**) and the corresponding height distributions (**d**, **e**, and **f** respectively) (see also **Table 2**).

Table 2. Height average of the nanofibers from the AFM images and transmittance of the suspensions at 0.1% and pH 3.

	Height average	Transmittance at 550 nm	Fine fraction
	nm	%	%
S-ChNF	9 ± 6	15.2 ± 0.6	17 ± 1
F-ChNF	11 ± 6	28.7 ± 0.8	27 ± 1
W-NF	10 ± 4	18.2 ± 0.5	1 ± 2

In summary, ChNFs were successfully prepared from all three sources, fly larvae, mealworm waste, and commercial shrimp shell chitin, having only small traces of proteins as noted by NMR spectra. The purification and fibrillation processes did not affect the chitin structure, resulting in highly *N*-acetylated ChNFs. The ChNF extracted from fly and shrimp were structurally similar, with no significant differences in terms of crystallinity, degree of *N*-acetylation, and charge density. One major difference was the presence of non-fully fibrillated species in S-ChNF, as shown by the low transmittance of the suspension and the fine-to-coarse ratio. Additional energy would be required to obtain a more homogeneous and finer S-ChNF.

W-NF consisted of 56 wt% chitin and 44 wt% cellulose, which is a result of the source biomass, a non-purified waste. Both polysaccharides were purified using the same purification steps leading to blended nanofibers. The negative surface charge of the cellulose fibers dominated the colloidal properties and resulted in negatively charged particles in suspension throughout a wide pH range. We could not identify the real state of the cellulosic colloids in the W-NF systems; however, it is likely that they were in the form of nanofibers given the AFM observation. The colloidal behavior at different pHs indicates that the surface of the nanofibers was dominated by cellulose, and that reactive amine groups do not contribute significantly. An advantage for future applications of the mealworm exuviae mixed waste is that both cellulose and chitin could be utilized as reactive moieties.

Film properties

Films were formed by overpressure filtration of ChNF suspensions followed by drying under two different conditions. One group of films was hot-pressed (HP) at 70 bar and 100 °C for 30 min and another was cold-pressed (CP), *i.e.,* dried overnight at room temperature under a much smaller pressure (0.012 bar). The density of the obtained films was similar and ranged from 1.2 to 1 g/cm^3, with that of cold-pressed ones being slightly higher (below 10% increase) than their hot-pressed counterparts. The transparency of the films depended both on the source and the processing conditions (**Figure 4a**). The transmittance at 550 nm for films obtained by cold (CP) and hot pressing (HP) ranged from 7.2 ± 0.5% to 0.8 ± 0.06% for S-ChNF and from 21 ± 2% to 1.8 ± 0.2% for F-ChNF, respectively (see **Figure 4b**). The opacity of the films was likely a result from the high structural porosity.[39] When the films were hot pressed, the speed of drying and water evaporation was considerably higher compared to that from overnight cold drying. Thus, the nanofibers in hot pressing had little time to rearrange and entangle, leaving a porous or defective structure in the packed lamellas. The F-ChNF CP film had higher transparency than the S-ChNF CP film, which was expected due to the higher homogeneity of F-ChNF and the smaller concentration of fiber aggregates in the suspension.

Water contact angles were measured for each film to gain insights into the surface energy of the different chitins. The films were highly hydrophilic, with contact angles ranging from 29 ± 0.3° to 40 ± 2° for S-ChNF HP and F-ChNF CP films, respectively. However, differences were noticed between the film-forming procedures: HP films trended towards lower contact angles due to their smoother surfaces in comparison with the CP counterparts. W-NF had a slightly higher contact angle compared to their shrimp and fly counterparts (**Figure 4c**). This is due to the presence of constituents of opposite surface charge (chitin and cellulose), leading to partial charge neutralization and fewer groups to possibly interact with water.[40] Consolidation of the

W-NF suspension at different pH did not alter the water contact angle, and neither the transmittance of the resulting films (**Figure 4**).

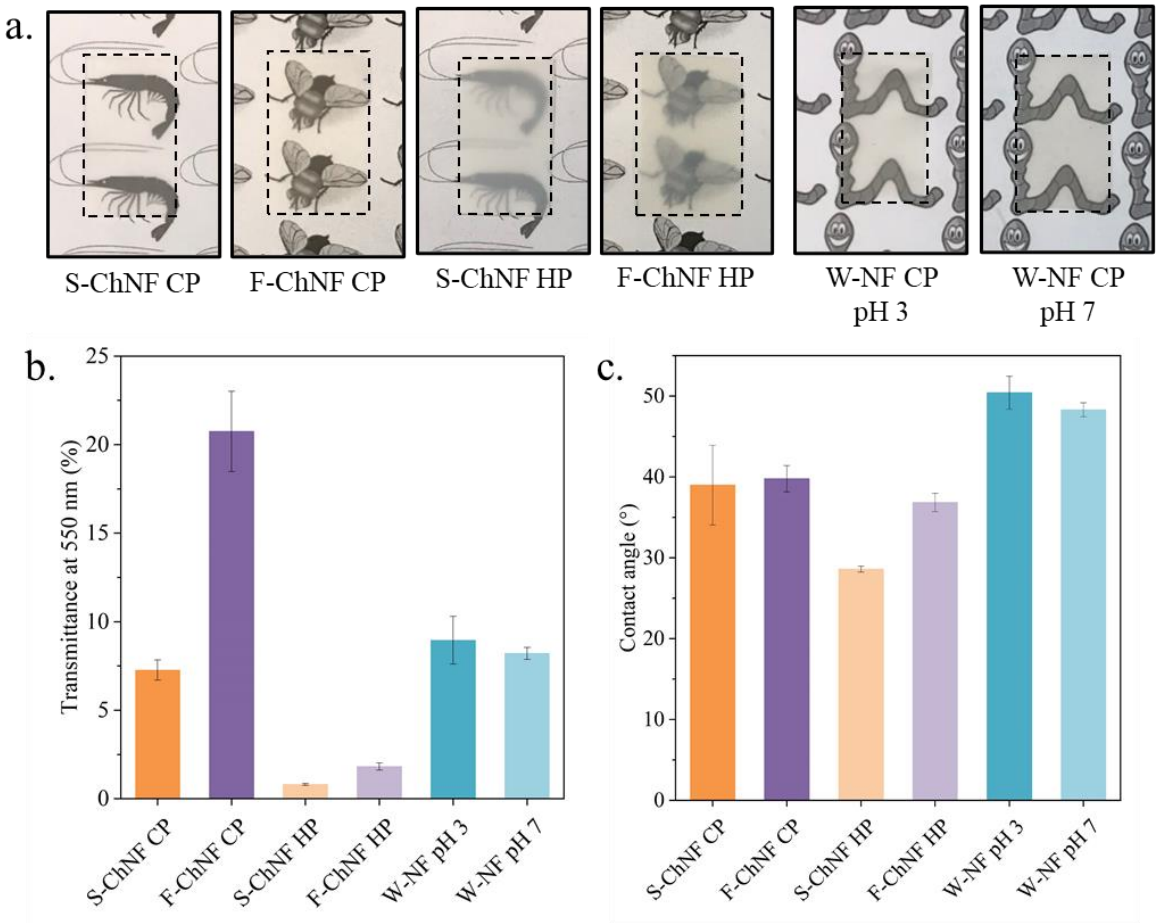

Figure 4. Images of the different films processed with cold (CP) or hot pressing (HP) at pH 3 or 7 for W-NF (**a**). Transmittances of the films measured by UV-Vis spectrophotometry (**b**) and contact angles measured 2 min after drop deposition (**c**).

All the films were subjected to tensile tests to evaluate their mechanical performances (**Figure 5**). Following the previous results, the strength of the chitinous nanofibrillar networks was influenced mostly by the assembling conditions (CP or HP) rather than by the nature of the chitin precursor. The HP process induced an increase in Young's modulus from 5.2 ± 0.7 GPa to 8.0 ± 0.2 GPa for S-ChNF and from 4.8 ± 0.4 GPa to 7.2 ± 0.3 GPa for F-ChNF. However,

the maximum tensile strain and hence the toughness were greatly reduced by the hot-pressing process, going from 5.5 ± 0.7% to 1.9 ± 0.2% for S-ChNF and from 5.0 ± 0.6% to 1.4 ± 0.1% for F-ChNF. The decrease in toughness could be explained by the reduced amount of water present in the films after the hot pressing. Indeed, water is known for its plasticizing role in cellulosic films. Sharma et al. showed that treatment of films at 100 °C or higher decreased the water retention of the film.[41] SEM images of the cross-sections of the films obtained after the tensile tests showed a paper-like structure, with fibers aligned in the plane and without visible aggregation of nanofibers (see **Figure 5b-c** and **Figure S5**).

W-NF, with its composite nature, was processed at pH 3 and 7, but only under cold-pressing conditions. As noted, CP offered products with superior mechanical properties compared to the films assembled from F-ChNF and S-ChNF. Two pH values were used to determine the effect of the amine protonation on the film properties. Even with a slightly higher toughness, given the higher elongation, the mechanical properties of the W-NF films were independent of the pH prevalent during film formation, as concluded from the variance of the results. In addition, the SEM image of the cross-section of the films did not show any clear difference with regard to porosity or nanofiber aggregation (**Figure 5c** and **S5**). Moreover, films from W-NF showed an elongation and toughness twice those observed for S-ChNF and F-ChNF. To better understand the mechanical properties of W-NF films, we produced a reference film containing 50 wt% of cellulose nanofibers (CNF) and 50% of ChNF and compared its mechanical properties to films of neat ChNF and CNF (see **Figure S6**). The CNF film showed higher toughness, Young's modulus, and tensile strength than the ChNF film. The film with 50:50 ChNF:CNF displayed intermediate properties, between those of CNF and ChNF. Therefore, one can speculate that the cellulose component in W-NF was not in the same state as traditional CNF, but possibly smaller or highly infused or entangled nanofibers. While the films from the ChNF:CNF mixture nearly followed the rule of mixtures, our W-NF displayed reinforcing

synergies between the chitin and cellulose components, given the better mechanical performance compared to the other chitin nanofibers.

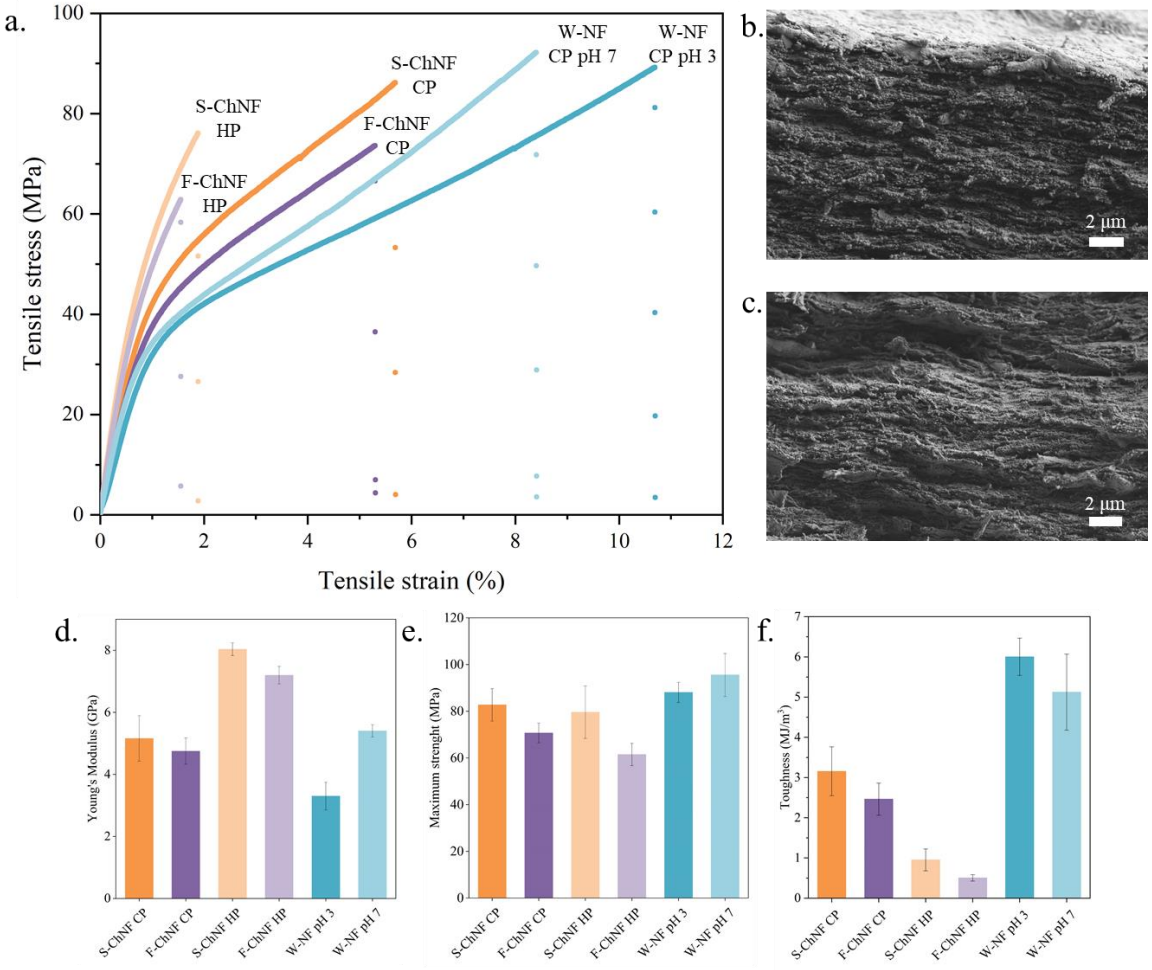

Figure 5. Tensile stress vs. strain profiles of the different films (**a**). Cross-section images of F-ChNF CP (**b**) and W-NF pH 7 (**c**). Young's Modulus (**d**), maximum strength (**e**) and toughness of the films (**f**).

The association of ChNF with other polymers, either towards new functionalities or enhanced properties of the films, has been considered. For instance, Zhang et al. showed that contact between cationic chitin nanocrystals and anionic TEMPO-oxidized CNF led to interfacial

complexation, allowing dry-spinning of microfibers.[42] The same phenomenon was observed by Grande et al. with deacetylated ChNF and anionic seaweed alginate, filaments with wet strength close to 50 MPa were obtained although the components were both hydrophilic.[43] Kim et al. achieved lower oxygen transmission rates using layer-by-layer (LbL) deposition on PET of CNF and chitin nanocrystals compared to the individual biopolymers. The nanoscale blending by LbL assembly led to synergies between the two polymers.[44] Therefore, our substrates present an alternative to explore a synergism between the nanofibrillar matrices, e.g., by taking advantage of W-NF, which contains both chitin and cellulose. Co-grinding biopolymers with nanofibers has been shown to lead to high-performance nanofibers, where the biopolymers are fully infused in the nanofibrillar matrix.[45] Moreover, it seems that the advantages arising from co-grinding techniques may also hold true for insoluble biocolloids, as it was the case of the resulting suspensions obtained by co-homogenization from the mealworm waste.

In summary, ChNF from insects showed similar properties than those obtained from shrimp, with additional features depending on the nature of the starting precursor. The method of film assembly was most relevant as far as the mechanical properties of the obtained films. Hence, the process needs to be chosen depending on the desired application.

Overall sustainability, insights on potential applications, and future prospects for insect-based ChNF

ChNFs present several application prospects, both as suspensions and films. For instance, ChNFs can kinetically stabilize oil-in-water Pickering emulsions at concentrations as low as 0.1 wt%, making them good candidates to replace petrochemical surfactants.[17,46] Mixtures of cellulose and chitin at different ratios have also been studied for Pickering stabilization and

resulted in super-stable emulsions.[47] ChNFs have also demonstrate their ability for high-barrier films or coatings.[48] Another way to valorize chitin from residual biomass is by complete or partial deacetylation into chitosan, which is soluble in water at mildly acidic pH and boasts applications in food packaging,[49] biomedical materials,[50] food additives *etc*.[16,51]

Also, some environmental aspects of using waste to produce ChNFs should be put forward here. This study shows that ChNFs from *Hermetia illucens* larvae have similar properties than ChNFs from shrimp shells. ChNF isolation from fishery waste is by common sense already sustainable, and we herein enable the isolation of this biocolloid from insects *via* an equally green (if not greener) procedure and propose its use in materials with superior performance. It is not among our goals, though, to indicate quantitatively which route is more sustainable, but to provide insights on their overall sustainability relying on qualitative indicators of environmental footprint (**Figure 6**).

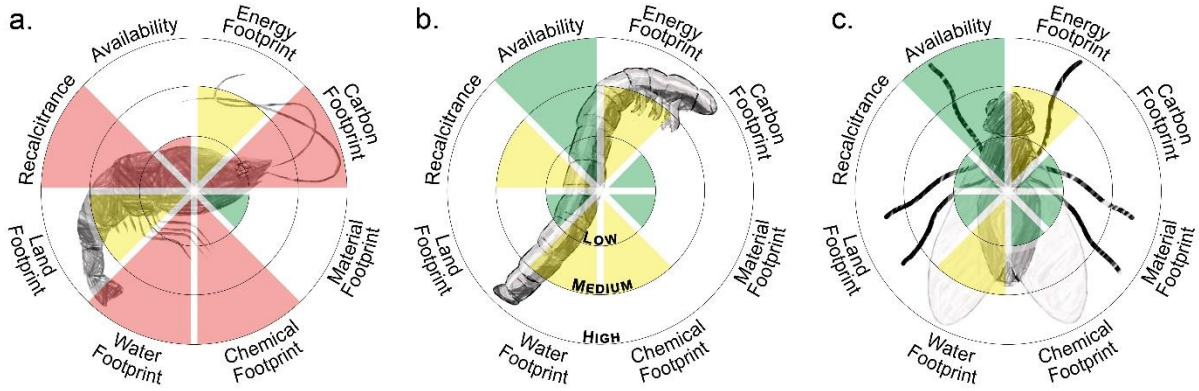

Figure 6. Overall qualitative evaluation of shrimp **(a)**, pupal exuviae **(b)**, and larval exoskeleton **(c)** sustainability as sources of nanochitin. *Availability* considers geographical restrictions, seasonality, and lifecycle duration for biomass generation. *Energy footprint* relates to any energy input in the production chain, renewable energy contributing less to the ultimate footprint than its fossil analogue. *Carbon footprint* encompasses emissions of greenhouse

gases, including carbon dioxide, methane, nitrous oxide, and ozone. *Material footprint* accounts for the depletion of natural resources for use in biomass generation and fractionation, while *chemical and water footprints* relate to emissions of chemicals and use of freshwater in these processes, respectively. Finally, *land footprint* translates the use of land to isolate nanochitin, including that for feed cultivation, to absorb the waste generated in the processes, and the land use change induced by a change in current practices. The levels (low, green; medium, yellow; high, red) were attributed in relative terms to illustrate qualitatively the comparison between the three scenarios, relying on our data and literature reports. Note that they are not meant to be compared with other procedures and goods (the carbon footprint of nanochitin isolation from shrimp is the highest among the three resources, but is significantly lower than that of livestock, as an example). Several of these indicators are intricately connected with biomass recalcitrance.

The starting biomasses can be compared in terms of availability, including geographical restrictions, seasonality, and lifecycle duration. Overall, insects reproduce at high rates and boast short maturation periods,[2] producing leftover streams that are abundant in chitin. Each mealworm female, for instance, reaches adulthood in 10 weeks and generates nearly 160 eggs throughout the 3-month lifespan.[5] In the case of BSF larvae, the transition to adulthood gives rise to chitin-rich larval exoskeletons (ecdysis) and pupal exuviae (skin renewal),[12] also at a high rate.[5] For shrimp, this cycle of course depends on species among other variables, but typically lasts for 7-8 months before harvesting, and 9-14 months until broodstock. Although important, the chitin yield is rather difficult to compare among the different sources as it varies with species, parts used for isolation, and the isolation protocol itself. Because of their short lifecycle and the growing insect economy, insect biomass appears more available.

Also relevant from the environmental angle is the biomass recalcitrance, which will affect not only extraction time, but also energy input, consumption of chemicals, and inevitably, costs.

Even if using an abundant, inexpensive waste, fractionation of crustacean shells is wasteful, expensive, and involves highly corrosive sodium hydroxide (for protein removal) and hydrochloric acid (for decomposition of calcium carbonate).[52] Insects comprise lower loads of minerals compared to crustacean shells (<6% *vs* 30-50%).[23] Yet, insect chitin may also be recalcitrant to some extent owing to sclerotization, *i.e.*, when proteins are covalently crosslinked to catecholic compounds and chitin.[12] This is true for pupal exuviae, but not for larval exoskeletons, making chitin isolation from the latter preferable.

Lower recalcitrance means not only less energy input, but also less use of harsh chemicals, including HCl, which has a negative impact on acidification of complex environments,[53] leaving behind a solid chemical footprint. The isolation of 1 kg chitin from shrimp shells requires *ca.* 2.5 kg of HCl and 1.3 kg of NaOH, plus 167 L of water.[53] HCl has been traditionally the acid of choice for the demineralization of crustacean shell-derived chitin, but milder, less corrosive acids (*e.g.*, formic acid) have been used for less recalcitrant larval exoskeletons.[12] Such a replacement is also relevant from the technical angle, as strong acid treatment is responsible for chitin depolymerization, hence milder acidic treatments from insect purification can lead to better preserved chitin fibers. Recovery and recyclability of the acid can also be developed as it is classically the case in industry. Moreover, new extraction processes with ionic liquid are emerging,[54] which are considered green solvents. It was demonstrated that chitin extracted with ionic had high molecular weight and high purity.

Importantly, the acid demineralization of the calcium carbonate-rich shrimp shells releases *ca.* 0.7 kg CO_2/kg chitin, this CO_2 being considered as of fossil origin.[53] Not only fractionation operations, but also logistics involved in the supply chain ought to be considered when assessing emissions. If CO_2 emission is to be avoided in the case of crabs and shrimps, the prevalent commercial sources of chitin, availability is concentrated in coastal regions as most species are marine.[12] Only shell transportation and bulldozer operations have been shown to

consume 20+ L diesel per ton of chitin,[53] although the emissions of greenhouse gases (GHG) in fisheries are dominated by feed production.[55] Insect farming, on the other hand, is globally suitable and has the great advantage of no geographical restrictions.[11] Additionally, the technological features of highly deacetylated chitin derived from insect depend neither on the geographical location nor on the organic substrate, as showcased for food waste-fed insects.[11] Indeed, organic (*e.g.*, agricultural and urban) waste is abundantly available all year-round, denoting another plus of insects over crustaceans as the chitin source. The global warming potential – typically expressed in CO_2-equivalents, considering CO_2, CH_4, and N_2O emissions, which is already low for mealworms (2.7 kg of CO_2-eq/kg edible protein) compared to other animals – may be further decreased in a straightforward fashion by using local leftover stream, as this indicator is dominated by production and transportation of feeding (*ca.* 56%) followed by gas and electricity for heating the rearing environment (*ca.* 43%).[5] When optimized, insects farms can become even carbon neutral or negative; their handprint could therefore be calculated to measure the positive impact of their production on the environment.[56]

While mealworms do not produce enteric CH_4,[57] *H. illucens* outstands owing to the ability of its larvae to digest organic matter. The biodigesting approach further fits the insect biorefinery into the circular bioeconomy by opening up the possibility of feeding larvae with nutritious agri-food side streams (*e.g.*, brewery spent grains and okara),[11] which may denote not only a major environmental issue but also an opportunity to upcycle food waste into economically valuable biomass,[58] including nanochitin. This also applies to municipal waste that, when decomposed by *H. illucens* larvae, will generate less malodors, potential diseases, and methane emission. Notably, between egg hatching and the prepupal stage (two weeks), *H. illucens* converts *ca.* 20 times their own weight of waste.[59] While most of worldwide commercialization of chitin derives from crustacean shells as by-product of the fishery industry, chitin isolation from organic leftover stream-fed insects can be consider a by-product of the by-product,

rendering a milder material footprint owing to the diminished extraction of raw materials from nature.

Whereas biogenic CO_2 emissions arising from degrading organic matter do not contribute to a net increase in atmospheric CO_2, as biogenic carbon is scavenged and released rapidly, biogenic CO_2 emissions resulting from land use change denotes a net addition to atmospheric CO_2.[53] The latter includes clearing of land for crop production. As mentioned above, mealworms can be fed organic waste, eliminating the need for feeding with crops. Although the land use for shrimp farming is virtually null when farming is extensive, there is an induced land use change (iLUC) associated with diverting its shells from their traditional use as animal feed. This iLUC, in turn, augments the need to deforest land for crop cultivation (further emitting CO_2) and/or to increase the yield in cultivated land using nitrogen fertilizers (boosting acidification).[53] When shrimp farming is intensive, additional land use due to earthen ponds and feed production should be considered.[55,60] The already low land footprint of insect farming can be further reduced by vertical farming.

This study has also demonstrated that a direct valorization of untreated waste from the mealworm industry, comprising chitin-rich exuviae and cellulose-rich rearing substrate, is viable and can lead to strong biobased films.

In a more sustainable perspective, partial purification of chitin could also be achieved giving rise to both energy and chemicals saving compared to complete purification as well as new properties due to the presence of impurities. For example, Nawawi et al.[26] extracted ChNF from mushroom with only partial removal of glucans to maintain the chitin-glucan complexes naturally present in mushrooms. Films with tensile strengths up to 200 MPa were produced and two times higher Young's moduli than for ChNF from crab were reported. Following the same idea, Ifuku et al. did not deproteinate chitin fibers from crab to yield protein-rich ChNF, which

displayed similar reinforcing properties than neat, highly purified ChNF.[61] Finally, one must consider the need for highly purified systems, as non-purified fibers have been performing similar, if not better, given natural synergies present on the precursors.

CONCLUSION

In this study, we prepared nanofibers from chitin-rich biomass. Chitin from fly larvae and an industrial mealworm waste stream were compared to that from commercially available chitin (from shrimp shells). Fly-derived chitin nanofibers (F-ChNF) showed similar properties compared to shrimp chitin nanofibers (S-ChNF), for example, in terms of crystallinity, degree of acetylation and film mechanical properties. Moreover, F-ChNF featured superior fibrillation behavior which resulted in suspensions with higher transmittance and produced films with higher transparency. In contrast, the nanofibers prepared from the mealworm waste (W-NF) differed considerably from the other samples, due to the presence of cellulose from feeding residues, which was incorporated in the form of composite nanofibers. The surface charge of the colloidal suspension was dominated by the cellulose component, explaining a colloidal stability over a large pH range. Films from W-NF were less brittle than the other ChNF films and had a higher toughness (double the value) than those from the F- and S-ChNF samples.

Taking all together, ChNF from fly larvae shows high promise as alternative to commercial chitin, but the valorization of mealworm waste as W-NF is expected to further open a new field of applications given the synergistic effects between the two components, chitin and cellulose. Our results demonstrate that side streams from the emerging insect industry can be valuable sources for future materials.

EXPERIMENTAL SECTION

Materials. Chitin flakes from shrimp were obtained from Sigma-Aldrich. Chitin from fly larvae (*Hermetia illucens*) was provided by S-Fly (France), and the chitinous waste from mealworm (*Tenebrio molitor*) farming was provided by Die Wurm Farm (Austria). All chitinous samples were received as dried powder. Bleached Kraft Hardwood pulp was used as never dried raw materials to produce the reference cellulose nanofibers (CNF) following microfluidization (M-110P, Microfluidics In., USA, 2000 bar with 200- and 100-μm chambers) using six passes and with no chemical pretreatment. All reagents and solvents were purchased from Sigma-Aldrich and used as received.

Chitin Purification. Chitin from fly and mealworm were first purified with a Soxhlet extraction with hexane for 6 h. Chitin purification was optimized following the procedure described by Percot at al.[28] First, acid hydrolysis at 0.25 M and room temperature was controlled following the increase of pH that occurred upon dissolution of calcium carbonate. In the same way, deproteinization with NaOH 1 M at 50 °C was controlled by UV absorption at 280 nm, characteristic of the tryptophan protein. A final bleaching step, with sodium chlorite at 80 °C for 2 h, was used to remove any residual pigments. Only one cycle was needed for the chitin from shrimp while three were needed to obtain white chitin from fly. Four bleaching cycles separated by sodium hydroxide purification step at 70 °C for 1 h were needed to obtain white chitin from the mealworm waste. The yield was calculated by dividing the final dry mass of the obtained material by the initial mass of the purified biomass.

Characterization of the raw and purified chitin flakes.

Purity. Solid state ^{13}C NMR was used to analyze the purity of the extracted chitinous fibers. Before measurement, fiber samples were hydrated in DI water for 24 h at room temperature and excess water was removed by squeezing the wet samples between tissue paper. Solid state

^{13}C NMR experiments were performed according to Beaumont et al.[62] on a Bruker Avance III HD 400 spectrometer (resonance frequency of ^{13}C of 100.61 MHz), equipped with a 4-mm dual broadband CP-MAS probe. The degree of acetylation was calculated by comparing the integrals of **C2** (51-58 ppm region) and **C**H_3 (acetyl) (21.3-23.7 ppm) peaks. The amount of cellulose in the mealworm sample was estimated by relating the integral of the **C2** with the **C1** (96-109 ppm region) peak.

Ash content. A thermogravimetric analyzer (Q500, TA instruments) was used to measure the ash content of the different samples before and after purification. For that purpose, 10 mg of biomass were dried and then carbonized at 600 °C for 15 min within an oxygen-containing atmosphere.

Nanofiber suspension preparation. The purified chitins were diluted to 0.6% and acidified with acetic acid to reach pH 3. The fibers were pre-treated with an Ultra-Turrax homogenizer (IKA, Germany) for 10 min at room temperature, then fibrillated with six passes in a microfluidizer (M-110P, Microfluidics In., USA) at 1500 bar using sequentially the 400- and 200-µm chambers. Nanochitin suspensions are herein referred to as S-ChNF, F-ChNF, and W-NF for the ChNF suspension coming respectively from shrimp, fly larvae, and chitinous waste from mealworm farming. Part of W-NF suspension was dialyzed (6-8 kDa membrane) in deionized water to obtain a suspension of neutral pH.

Suspension characterization. *Chemical structure*. To analyze the changes in chemical structure of the fibers after purification and fibrillation, Fourier-transform infrared (FTIR) spectra were acquired on a Perkin Elmer spectrometer in ATR mode. Samples were dried at 105 °C before analyses. The resolution was 2 cm^{-1} and the spectra shown are the cumulative data after at least 10 scans.

Surface charge measurement. Zeta potential of the nanofibers suspensions at different pH was measured with a Malvern Zetasizer Nano using a dip cell. The suspensions were diluted to 0.05% and pH was adjusted with NaOH and HCl or buffer solutions, conductivity was corrected with NaCl 1 M to 0.25 mS/cm. At least duplicate samples were analyzed.

Conductometric titrations were done with an automatic titrator (Metrohm). Before titration, nanofiber suspensions were dialyzed as described above to remove acetic acid. Then, 0.1 g of nanofibers were dispersed in 100 mL water, 0.2 mL HCl 0.1 M, and 0.1 mL NaCl 0.5 M were added. The suspension was then titrated against NaOH 0.02 M at 0.1 mL/min and the conductivity was measured under continuous magnetic stirring. The surface charge was calculated from the volume of NaOH added corresponding to the difference between the two inflection points representing the change in conductivity of the solution (V_{eq}). The degree of acetylation (DA) of the suspensions was then calculated using the equation below:

$$DA = 1 - \frac{M_a}{M_a - M_d + \frac{m}{[NaOH] \times V_{eq}}} \quad (1)$$

where *m* represents the mass of nanofibers and M_a and M_d correspond to the molar mass of the acetylated (203 g/mol) and deacetylated (161 g/mol) chitin.

Morphology. The morphology of the nanofibers was analyzed with atomic force microscopy (Bruker MultiMode 8 AFM). For sample preparation, PEI was drop cast on silica substrates, after 1 min contact, the substrate was rinsed and then dipped in diluted nanofiber suspension (0.001 wt%) to deposit nanofibers on the surface. NanoScope Anaylsis software was used to measure the fibers height. At least 50 different nanofibers were measured, and the average was calculated.

UV-Vis transmittance of suspension at pH 3 and 0.1% was measured with a spectrophotometer (Shimadzu UV-2550) to obtain information on the fiber's behavior in suspension. To obtain a

ratio of fine fibers, the suspensions were diluted to 0.1% and centrifuged at 3000 rpm (4.2 x g) for 15 min.[63] Then, the supernatant was removed and weighted. The ratio of fines was calculated following the equation below:

$$Fines\ (\%) = \frac{m_{sup}}{m_{tot}} \times 100 \qquad (2)$$

where m_{sup} represents the mass of nanofibers in the supernatant and m_{tot} the total mass of initial nanofibers. The measurement was performed in triplicate.

Film preparation. Films (30 g/m^2) were produced using a positive pressure filtration unit with 0.45-µm PVDF membranes. To better understand the role of the drying process, some films were hot pressed (HP) at 100 °C and 70 bar for 30 min and others cold-pressed with a 3.4 kg load (0.012 bar) and dried overnight at room temperature. Films were processed at pH 3 and for the W-NF sample, one additional film was made at pH 7 after dialysis of the suspension.

Films containing CNF. To better understand the mechanical behavior of the W-NF films, a film with 50 wt% of S-ChNF and CNF was prepared. For that purpose, the desired mass of nanofibers was weighted and mixed with an Ultra-Turrax homogenizer for 5 min at room temperature followed by over-pressure filtration and cold pressing and drying overnight at room temperature, using the same conditions than those use for the chitin films. A film containing only CNF was also processed.

Film characterization. *Density.* The density of the films was measured gravimetrically by weighting the films at 23 °C and 50% relative humidity and measuring their thicknesses and surfaces in the same conditions.

Crystallinity. X-ray diffraction pattern of the chitin films was measured, and their crystallinity indexes were calculated. Rigaku Smart-Lab diffractometer with Cu anode operated at 45 kV and 200 mA was used to measure the X-ray diffraction intensities between 5 and 65° in 2Θ.

Films of ChNF were dried at 105 °C overnight before measurement in reflection mode. The crystallinity index was calculated following Càrdenas et al.[30] method using the ratio between the crystalline peak intensity at 19.2° corresponding to the (110) diffraction plan and the amorphous part at 12.6°. The crystalline index was then calculated with the following equation:

$$CI = \frac{(I_{110} - I_{am})}{I_{110}} \times 100 \quad (3)$$

Morphology. Scanning electron microscopy (SEM) images of the cross-sections after mechanical tests were made to observe the homogeneity of the films. Zeiss, Sigma VP SEM was operated at 1.5 kV. A 4-nm-thick Au/Pd layer was sputtered on the sample before analysis. Most representative SEM images were selected for the discussion among at least 10 images in different zones of observation.

Wettability. Contact angle of the films was measured with a Theta Flex optical tensiometer (Biolin Scientific) using 5-µL drops. The recorded contact angles were measured after 120 s of drop contact on different zones. At least triplicate was performed.

Transparency. A UV-Vis spectrophotometer (Shimadzu UV-2550) was utilized to measure the transparency of the films between 200 and 800 nm. The average of triplicate is proposed for discussion.

Mechanical properties. Tensile tests of 50 x 5 mm^2 samples were carried out on an Instron 5944 with a 2-kN load cell at 1 mm/min with an initial gap of 30 mm. Before measurements, specimen thicknesses and width were measured with a micrometer and a caliper, respectively. Every sample was conditioned at 23 °C and 50% relative humidity for at least 24 h before and during the measurements. At least triplicate was performed for each film.

SUPPORTING INFORMATION

FTIR of raw materials, ^{13}C NMR spectra of the raw materials, ^{13}C NMR spectrum of the purified mealworm sample, assignation table of IR peaks, zeta potential as function of pH, SEM cross-section images of films, tensile stress versus strain profiles of CNF film, mix of 50% S-ChNF and 50% CNF film, S-ChNF CP and W-NF pH 3.

ACKNOWLEDGEMENTS

The authors would like to thank S-Fly and Die Wurm Farm for providing the raw materials needed for this study and Tuyen Nguyen for the fluidization of the different ChNFs. LGP2 is part of the LabEx Tec 21 (Investissements d'Avenir - grant agreement n°ANR-11-LABX-0030) and of PolyNat Carnot Institute (Investissements d'Avenir - grant agreement n° ANR-16-CARN-0025-01). This work was supported by Grenoble INP, "Bourse Présidence" and the European Research Council (ERC) under the European Union's Horizon 2020 research and innovation programme (grant agreement No 788489). O.J.R. also acknowledges the Canada Excellence Research Chair initiative, and the Canada Foundation for Innovation (CFI). The support by the Austrian Biorefinery Center Tulln (ABCT) is gratefully acknowledged.

REFERENCES

(1) Payne, C. L. R.; Scarborough, P.; Rayner, M.; Nonaka, K. Are Edible Insects More or Less 'Healthy' than Commonly Consumed Meats? A Comparison Using Two Nutrient Profiling Models Developed to Combat over- and Undernutrition. *European Journal of Clinical Nutrition* **2016**, *70* (3), 285–291. https://doi.org/10.1038/ejcn.2015.149.

(2) Parodi, A.; Leip, A.; De Boer, I. J. M.; Slegers, P. M.; Ziegler, F.; Temme, E. H. M.; Herrero, M.; Tuomisto, H.; Valin, H.; Van Middelaar, C. E.; Van Loon, J. J. A.; Van Zanten, H. H. E. The Potential of Future Foods for Sustainable and Healthy Diets. *Nature Sustainability* **2018**, *1* (12), 782–789. https://doi.org/10.1038/s41893-018-0189-7.

(3) McClements, D. J. *Future Foods: How Modern Science Is Transforming the Way We Eat*; Copernicus, 2019. https://doi.org/10.1007/978-3-030-12995-8.

(4) Sánchez-Muros, M.-J.; Barroso, F. G.; Manzano-Agugliaro, F. Insect Meal as Renewable Source of Food for Animal Feeding: A Review. *Journal of Cleaner Production* **2014**, *65*, 16–27. https://doi.org/10.1016/j.jclepro.2013.11.068.

(5) Oonincx, D. G. A. B.; Boer, I. J. M. Environmental Impact of the Production of Mealworms as a Protein Source for Humans – A Life Cycle Assessment. *PLOS ONE* **2012**, *7* (12), e51145. https://doi.org/10.1371/journal.pone.0051145.

(6) Varelas, V. Food Wastes as a Potential New Source for Edible Insect Mass Production for Food and Feed: A Review. *Fermentation* **2019**, *5* (3), 81. https://doi.org/10.3390/fermentation5030081.
(7) Houben, D.; Daoulas, G.; Faucon, M.-P.; Dulaurent, A.-M. Potential Use of Mealworm Frass as a Fertilizer: Impact on Crop Growth and Soil Properties. *Scientific Reports* **2020**, *10* (1), 4659. https://doi.org/10.1038/s41598-020-61765-x.
(8) Rosa, R.; Spinelli, R.; Neri, P.; Pini, M.; Barbi, S.; Montorsi, M.; Maistrello, L.; Marseglia, A.; Caligiani, A.; Ferrari, A. M. Life Cycle Assessment of Chemical vs Enzymatic-Assisted Extraction of Proteins from Black Soldier Fly Prepupae for the Preparation of Biomaterials for Potential Agricultural Use. *ACS Sustainable Chem. Eng.* **2020**, *8* (39), 14752–14764. https://doi.org/10.1021/acssuschemeng.0c03795.
(9) Spranghers, T.; Ottoboni, M.; Klootwijk, C.; Ovyn, A.; Deboosere, S.; Meulenaer, B. D.; Michiels, J.; Eeckhout, M.; Clercq, P. D.; Smet, S. D. Nutritional Composition of Black Soldier Fly (Hermetia Illucens) Prepupae Reared on Different Organic Waste Substrates. *Journal of the Science of Food and Agriculture* **2017**, *97* (8), 2594–2600. https://doi.org/10.1002/jsfa.8081.
(10) Hahn, T.; Roth, A.; Febel, E.; Fijalkowska, M.; Schmitt, E.; Arsiwalla, T.; Zibek, S. New Methods for High-Accuracy Insect Chitin Measurement. *Journal of the Science of Food and Agriculture* **2018**, *98* (13), 5069–5073. https://doi.org/10.1002/jsfa.9044.
(11) Sanandiya, N. D.; Ottenheim, C.; Phua, J. W.; Caligiani, A.; Dritsas, S.; Fernandez, J. G. Circular Manufacturing of Chitinous Bio-Composites via Bioconversion of Urban Refuse. *Sci Rep* **2020**, *10* (1), 1–8. https://doi.org/10.1038/s41598-020-61664-1.
(12) Hahn, T.; Roth, A.; Ji, R.; Schmitt, E.; Zibek, S. Chitosan Production with Larval Exoskeletons Derived from the Insect Protein Production. *Journal of Biotechnology* **2020**, *310*, 62–67. https://doi.org/10.1016/j.jbiotec.2019.12.015.
(13) Song, Y.-S.; Kim, M.-W.; Moon, C.; Seo, D.-J.; Han, Y. S.; Jo, Y. H.; Noh, M. Y.; Park, Y.-K.; Kim, S.-A.; Kim, Y. W.; Jung, W.-J. Extraction of Chitin and Chitosan from Larval Exuvium and Whole Body of Edible Mealworm, Tenebrio Molitor. *Entomological Research* **2018**, *48* (3), 227–233. https://doi.org/10.1111/1748-5967.12304.
(14) Salaberria, A. M.; Labidi, J.; Fernandes, S. C. M. Different Routes to Turn Chitin into Stunning Nano-Objects. *European Polymer Journal* **2015**, *68*, 503–515. https://doi.org/10.1016/j.eurpolymj.2015.03.005.
(15) Biswas, S. K.; Shams, Md. I.; Das, A. K.; Islam, Md. N.; Nazhad, M. M. Flexible and Transparent Chitin/Acrylic Nanocomposite Films with High Mechanical Strength. *Fibers Polym* **2015**, *16* (4), 774–781. https://doi.org/10.1007/s12221-015-0774-6.
(16) Ahmad, S. I.; Ahmad, R.; Khan, Mohd. S.; Kant, R.; Shahid, S.; Gautam, L.; Hasan, G. M.; Hassan, Md. I. Chitin and Its Derivatives: Structural Properties and Biomedical Applications. *International Journal of Biological Macromolecules* **2020**, *164*, 526–539. https://doi.org/10.1016/j.ijbiomac.2020.07.098.
(17) Zhu, Y.; Huan, S.; Bai, L.; Ketola, A.; Shi, X.; Zhang, X.; Ketoja, J. A.; Rojas, O. J. High Internal Phase Oil-in-Water Pickering Emulsions Stabilized by Chitin Nanofibrils: 3D Structuring and Solid Foams. *ACS Appl. Mater. Interfaces* **2020**, *12*, 11240–11251. https://doi.org/10.1021/acsami.9b23430.
(18) Ifuku, S.; Morooka, S.; Morimoto, M.; Saimoto, H. Acetylation of Chitin Nanofibers and Their Transparent Nanocomposite Films. *Biomacromolecules* **2010**, *11* (5), 1326–1330. https://doi.org/10.1021/bm100109a.
(19) Fan, Y.; Saito, T.; Isogai, A. Preparation of Chitin Nanofibers from Squid Pen β-Chitin by Simple Mechanical Treatment under Acid Conditions. *Biomacromolecules* **2008**, *9* (7), 1919–1923. https://doi.org/10.1021/bm800178b.
(20) Ifuku, S.; Nomura, R.; Morimoto, M.; Saimoto, H. Preparation of Chitin Nanofibers from Mushrooms. *Materials* **2011**, *4* (8), 1417–1425. https://doi.org/10.3390/ma4081417.

(21) Morin, A.; Dufresne, A. Nanocomposites of Chitin Whiskers from Riftia Tubes and Poly(Caprolactone). *Macromolecules* **2002**, *35* (6), 2190–2199. https://doi.org/10.1021/ma011493a.
(22) Kaya, M.; Baublys, V.; Can, E.; Šatkauskienė, I.; Bitim, B.; Tubelytė, V.; Baran, T. Comparison of Physicochemical Properties of Chitins Isolated from an Insect (Melolontha Melolontha) and a Crustacean Species (Oniscus Asellus). *Zoomorphology* **2014**, *133* (3), 285–293. https://doi.org/10.1007/s00435-014-0227-6.
(23) Huet, G.; Hadad, C.; Husson, E.; Laclef, S.; Lambertyn, V.; Araya Farias, M.; Jamali, A.; Courty, M.; Alayoubi, R.; Gosselin, I.; Sarazin, C.; Van Nhien, A. N. Straightforward Extraction and Selective Bioconversion of High Purity Chitin from Bombyx Eri Larva: Toward an Integrated Insect Biorefinery. *Carbohydrate Polymers* **2020**, *228*, 115382. https://doi.org/10.1016/j.carbpol.2019.115382.
(24) Brigode, C.; Hobbi, P.; Jafari, H.; Verwilghen, F.; Baeten, E.; Shavandi, A. Isolation and Physicochemical Properties of Chitin Polymer from Insect Farm Side Stream as a New Source of Renewable Biopolymer. *Journal of Cleaner Production* **2020**, *275*, 122924. https://doi.org/10.1016/j.jclepro.2020.122924.
(25) Hahn, T.; Tafi, E.; Paul, A.; Salvia, R.; Falabella, P.; Zibek, S. Current State of Chitin Purification and Chitosan Production from Insects. *Journal of Chemical Technology & Biotechnology* **2020**, *95* (11), 2775–2795. https://doi.org/10.1002/jctb.6533.
(26) Fazli Wan Nawawi, W. M.; Lee, K.-Y.; Kontturi, E.; Murphy, R. J.; Bismarck, A. Chitin Nanopaper from Mushroom Extract: Natural Composite of Nanofibers and Glucan from a Single Biobased Source. *ACS Sustainable Chem. Eng.* **2019**, *7* (7), 6492–6496. https://doi.org/10.1021/acssuschemeng.9b00721.
(27) Turck, D.; Castenmiller, J.; Henauw, S. D.; Hirsch-Ernst, K. I.; Kearney, J.; Maciuk, A.; Mangelsdorf, I.; McArdle, H. J.; Naska, A.; Pelaez, C.; Pentieva, K.; Siani, A.; Thies, F.; Tsabouri, S.; Vinceti, M.; Cubadda, F.; Frenzel, T.; Heinonen, M.; Marchelli, R.; Neuhäuser-Berthold, M.; Poulsen, M.; Maradona, M. P.; Schlatter, J. R.; Loveren, H. van; Ververis, E.; Knutsen, H. K. Safety of Dried Yellow Mealworm (Tenebrio Molitor Larva) as a Novel Food Pursuant to Regulation (EU) 2015/2283. *EFSA Journal* **2021**, *19* (1), e06343. https://doi.org/10.2903/j.efsa.2021.6343.
(28) Percot, A.; Viton, C.; Domard, A. Optimization of Chitin Extraction from Shrimp Shells. *Biomacromolecules* **2003**, *4* (1), 12–18. https://doi.org/10.1021/bm025602k.
(29) King, C.; Stein, R. S.; Shamshina, J. L.; Rogers, R. D. Measuring the Purity of Chitin with a Clean, Quantitative Solid-State NMR Method. *ACS Sustainable Chem. Eng.* **2017**, *5* (9), 8011–8016. https://doi.org/10.1021/acssuschemeng.7b01589.
(30) Cárdenas, G.; Cabrera, G.; Taboada, E.; Miranda, S. P. Chitin Characterization by SEM, FTIR, XRD, and 13C Cross Polarization/Mass Angle Spinning NMR. *Journal of Applied Polymer Science* **2004**, *93* (4), 1876–1885. https://doi.org/10.1002/app.20647.
(31) Waśko, A.; Bulak, P.; Polak-Berecka, M.; Nowak, K.; Polakowski, C.; Bieganowski, A. The First Report of the Physicochemical Structure of Chitin Isolated from Hermetia Illucens. *International Journal of Biological Macromolecules* **2016**, *92*, 316–320. https://doi.org/10.1016/j.ijbiomac.2016.07.038.
(32) French, A. D. Idealized Powder Diffraction Patterns for Cellulose Polymorphs. *Cellulose* **2014**, *21* (2), 885–896. https://doi.org/10.1007/s10570-013-0030-4.
(33) Lu, Y.; Sun, Q.; She, X.; Xia, Y.; Liu, Y.; Li, J.; Yang, D. Fabrication and Characterisation of α-Chitin Nanofibers and Highly Transparent Chitin Films by Pulsed Ultrasonication. *Carbohydrate Polymers* **2013**, *98* (2), 1497–1504. https://doi.org/10.1016/j.carbpol.2013.07.038.
(34) Yang, R.; Su, Y.; Aubrecht, K. B.; Wang, X.; Ma, H.; Grubbs, R. B.; Hsiao, B. S.; Chu, B. Thiol-Functionalized Chitin Nanofibers for As (III) Adsorption. *Polymer* **2015**, *60*, 9–17. https://doi.org/10.1016/j.polymer.2015.01.025.

(35) Lamarque, G.; Viton, C.; Domard, A. Comparative Study of the First Heterogeneous Deacetylation of α- and β-Chitins in a Multistep Process. *Biomacromolecules* **2004**, *5* (3), 992–1001. https://doi.org/10.1021/bm034498j.
(36) Shak, K. P. Y.; Pang, Y. L.; Mah, S. K. Nanocellulose: Recent Advances and Its Prospects in Environmental Remediation. *Beilstein J Nanotechnol* **2018**, *9*, 2479–2498. https://doi.org/10.3762/bjnano.9.232.
(37) Ifuku, S.; Nogi, M.; Abe, K.; Yoshioka, M.; Morimoto, M.; Saimoto, H.; Yano, H. Preparation of Chitin Nanofibers with a Uniform Width as α-Chitin from Crab Shells. *Biomacromolecules* **2009**, *10* (6), 1584–1588. https://doi.org/10.1021/bm900163d.
(38) Marei, N. H.; El-Samie, E. A.; Salah, T.; Saad, G. R.; Elwahy, A. H. M. Isolation and Characterization of Chitosan from Different Local Insects in Egypt. *International Journal of Biological Macromolecules* **2016**, *82*, 871–877. https://doi.org/10.1016/j.ijbiomac.2015.10.024.
(39) Toivonen, M. S.; Onelli, O. D.; Jacucci, G.; Lovikka, V.; Rojas, O. J.; Ikkala, O.; Vignolini, S. Anomalous-Diffusion-Assisted Brightness in White Cellulose Nanofibril Membranes. *Advanced Materials* **2018**, *30* (16), 1704050. https://doi.org/10.1002/adma.201704050.
(40) Toivonen, M. S.; Kurki-Suonio, S.; Schacher, F. H.; Hietala, S.; Rojas, O. J.; Ikkala, O. Water-Resistant, Transparent Hybrid Nanopaper by Physical Cross-Linking with Chitosan. *Biomacromolecules* **2015**, *16* (3), 1062–1071. https://doi.org/10.1021/acs.biomac.5b00145.
(41) Sharma, S.; Zhang, X.; Nair, S. S.; Ragauskas, A.; Zhu, J.; Deng, Y. Thermally Enhanced High Performance Cellulose Nano Fibril Barrier Membranes. *RSC Adv.* **2014**, *4* (85), 45136–45142. https://doi.org/10.1039/C4RA07469F.
(42) Zhang, K.; Ketterle, L.; Järvinen, T.; Hong, S.; Liimatainen, H. Conductive Hybrid Filaments of Carbon Nanotubes, Chitin Nanocrystals and Cellulose Nanofibers Formed by Interfacial Nanoparticle Complexation. *Materials & Design* **2020**, *191*, 108594. https://doi.org/10.1016/j.matdes.2020.108594.
(43) Grande, R.; Bai, L.; Wang, L.; Xiang, W.; Ikkala, O.; Carvalho, A. J. F.; Rojas, O. J. Nanochitins of Varying Aspect Ratio and Properties of Microfibers Produced by Interfacial Complexation with Seaweed Alginate. *ACS Sustainable Chem. Eng.* **2020**, *8* (2), 1137–1145. https://doi.org/10.1021/acssuschemeng.9b06099.
(44) Kim, T.; Tran, T. H.; Hwang, S. Y.; Park, J.; Oh, D. X.; Kim, B.-S. Crab-on-a-Tree: All Biorenewable, Optical and Radio Frequency Transparent Barrier Nanocoating for Food Packaging. *ACS Nano* **2019**, *13* (4), 3796–3805. https://doi.org/10.1021/acsnano.8b08522.
(45) Missio, A. L.; Mattos, B. D.; Otoni, C. G.; Gentil, M.; Coldebella, R.; Khakalo, A.; Gatto, D. A.; Rojas, O. J. Cogrinding Wood Fibers and Tannins: Surfactant Effects on the Interactions and Properties of Functional Films for Sustainable Packaging Materials. *Biomacromolecules* **2020**, *21* (5), 1865–1874. https://doi.org/10.1021/acs.biomac.9b01733.
(46) Bai, L.; Huan, S.; Xiang, W.; Liu, L.; Yang, Y.; Nugroho, R. W. N.; Fan, Y.; Rojas, O. J. Self-Assembled Networks of Short and Long Chitin Nanoparticles for Oil/Water Interfacial Superstabilization. *ACS Sustainable Chem. Eng.* **2019**, *7* (7), 6497–6511. https://doi.org/10.1021/acssuschemeng.8b04023.
(47) Lv, S.; Zhou, H.; Bai, L.; Rojas, O. J.; McClements, D. J. Development of Food-Grade Pickering Emulsions Stabilized by a Mixture of Cellulose Nanofibrils and Nanochitin. *Food Hydrocolloids* **2021**, *113*, 106451. https://doi.org/10.1016/j.foodhyd.2020.106451.
(48) Fan, Y.; Fukuzumi, H.; Saito, T.; Isogai, A. Comparative Characterization of Aqueous Dispersions and Cast Films of Different Chitin Nanowhiskers/Nanofibers. *International Journal of Biological Macromolecules* **2012**, *50* (1), 69–76. https://doi.org/10.1016/j.ijbiomac.2011.09.026.
(49) Wang, H.; Qian, J.; Ding, F. Emerging Chitosan-Based Films for Food Packaging Applications. *J. Agric. Food Chem.* **2018**, *66* (2), 395–413. https://doi.org/10.1021/acs.jafc.7b04528.

(50) Santos, V. P.; Marques, N. S. S.; Maia, P. C. S. V.; Lima, M. A. B. de; Franco, L. de O.; Campos-Takaki, G. M. de. Seafood Waste as Attractive Source of Chitin and Chitosan Production and Their Applications. *International Journal of Molecular Sciences* **2020**, *21* (12), 4290. https://doi.org/10.3390/ijms21124290.
(51) Younes, I.; Rinaudo, M. Chitin and Chitosan Preparation from Marine Sources. Structure, Properties and Applications. *Marine Drugs* **2015**, *13* (3), 1133–1174. https://doi.org/10.3390/md13031133.
(52) Yan, N.; Chen, X. Sustainability: Don't Waste Seafood Waste. *Nature* **2015**, *524* (7564), 155–157. https://doi.org/10.1038/524155a.
(53) Muñoz, I.; Rodríguez, C.; Gillet, D.; M. Moerschbacher, B. Life Cycle Assessment of Chitosan Production in India and Europe. *Int J Life Cycle Assess* **2018**, *23* (5), 1151–1160. https://doi.org/10.1007/s11367-017-1290-2.
(54) Shamshina, J. L.; Barber, P. S.; Gurau, G.; Griggs, C. S.; Rogers, R. D. Pulping of Crustacean Waste Using Ionic Liquids: To Extract or Not To Extract. *ACS Sustainable Chem. Eng.* **2016**, *4* (11), 6072–6081. https://doi.org/10.1021/acssuschemeng.6b01434.
(55) Cao, L.; Diana, J. S.; Keoleian, G. A.; Lai, Q. Life Cycle Assessment of Chinese Shrimp Farming Systems Targeted for Export and Domestic Sales. *Environ. Sci. Technol.* **2011**, *45* (15), 6531–6538. https://doi.org/10.1021/es104058z.
(56) Pajula, T.; Vatanen, S.; Behm, K.; Grönman, K.; Lakanen, L.; Kasurinen, H.; Soukka, R. *Carbon Handprint Guide: V. 2.0 Applicable for Environmental Handprint*; VTT Technical Research Centre of Finland, 2021; p 28.
(57) Oonincx, D. G. A. B.; Itterbeeck, J. van; Heetkamp, M. J. W.; Brand, H. van den; Loon, J. J. A. van; Huis, A. van. An Exploration on Greenhouse Gas and Ammonia Production by Insect Species Suitable for Animal or Human Consumption. *PLOS ONE* **2010**, *5* (12), e14445. https://doi.org/10.1371/journal.pone.0014445.
(58) Otoni, C. G.; Azeredo, H. M. C.; Mattos, B. D.; Beaumont, M.; Correa, D. S.; Rojas, O. J. The Food–Materials Nexus: Next Generation Bioplastics and Advanced Materials from Agri-Food Residues. *Advanced Materials* **2021**, 2102520. https://doi.org/10.1002/adma.202102520.
(59) Gao, Z.; Wang, W.; Lu, X.; Zhu, F.; Liu, W.; Wang, X.; Lei, C. Bioconversion Performance and Life Table of Black Soldier Fly (Hermetia Illucens) on Fermented Maize Straw. *Journal of Cleaner Production* **2019**, *230*, 974–980. https://doi.org/10.1016/j.jclepro.2019.05.074.
(60) Järviö, N.; Henriksson, P. J. G.; Guinée, J. B. Including GHG Emissions from Mangrove Forests LULUC in LCA: A Case Study on Shrimp Farming in the Mekong Delta, Vietnam. *Int J Life Cycle Assess* **2018**, *23* (5), 1078–1090. https://doi.org/10.1007/s11367-017-1332-9.
(61) Ifuku, S.; Urakami, T.; Izawa, H.; Morimoto, M.; Saimoto, H. Preparation of a Protein–Chitin Nanofiber Complex from Crab Shells and Its Application as a Reinforcement Filler or Substrate for Biomineralization. *RSC Adv.* **2015**, *5* (79), 64196–64201. https://doi.org/10.1039/C5RA12761K.
(62) Beaumont, M.; Rennhofer, H.; Opietnik, M.; Lichtenegger, H. C.; Potthast, A.; Rosenau, T. Nanostructured Cellulose II Gel Consisting of Spherical Particles. *ACS Sustainable Chem. Eng.* **2016**, *4* (8), 4424–4432. https://doi.org/10.1021/acssuschemeng.6b01036.
(63) Desmaisons, J.; Boutonnet, E.; Rueff, M.; Dufresne, A.; Bras, J. A New Quality Index for Benchmarking of Different Cellulose Nanofibrils. *Carbohydrate Polymers* **2017**, *174*, 318–329. https://doi.org/10.1016/j.carbpol.2017.06.032.

For Table of Contents Use Only

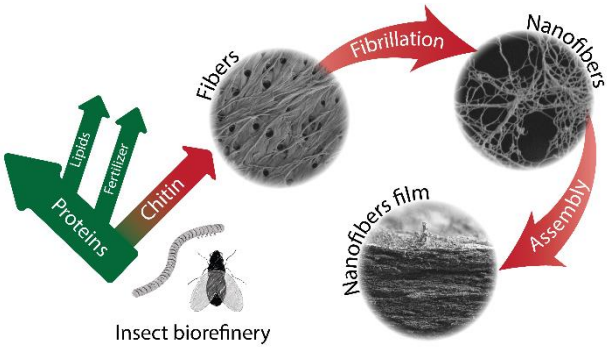

Synopsis:

Biomass derived from industrial insect farming is exploited as an emergent source of chitin nanofibers.